

# Plausible global emissions scenario for 2 °C aligned with China's net-zero pathway

Received: 7 November 2024

Accepted: 5 August 2025

Published online: 29 August 2025

 Check for updates

Junting Zhong<sup>1,2</sup>, Xiaoye Zhang<sup>1,2</sup> , Da Zhang <sup>2,3,4</sup>, Deying Wang<sup>1</sup>, Lifeng Guo<sup>1</sup>, Hantang Peng<sup>3</sup>, Xiaodan Huang<sup>3</sup>, Zhili Wang <sup>1</sup>, Yadong Lei <sup>1</sup>, Yixiong Lu <sup>5</sup>, Chenfei Qu<sup>3</sup>, Xiliang Zhang <sup>2,3,4</sup> & Changhong Miao<sup>2</sup>

Due to sizeable anthropogenic CO<sub>2</sub> emissions, China's transition towards carbon neutrality will reshape global CO<sub>2</sub> emissions, offering insights into warming levels, extreme events, overshoot, tipping points, and regional climate impacts. Here we develop an interdisciplinary and multi-model framework integrating up-to-date emissions inventory and China's net-zero pathway to construct a reality-aligned, sector-specific combined scenario (SSP2-com) for greenhouse gases and air pollutants across global-to-regional, national-to-provincial, and multi-resolution-grid scales. SSP2-com projects CO<sub>2</sub> peaking in concentration globally by 2062, and achieving net-zero emissions by 2072, driven by Asia-Pacific—particularly China—via energy and industrial reductions. Climate emulators show global temperatures initially track SSP2-4.5 but later diverge onto a distinct trajectory, reaching 2.01 °C by 2100 (~3.2 Watt m<sup>-2</sup>) and dropping below 2 °C within the first post-2100 decade, relevant to the Paris Agreement target. We further propose an evolving SSP2-com+ framework with updated trajectories to enhance timely alignment and cooperation. Our findings indicate balanced, nationally-determined decarbonization can stabilize warming near 2 °C without early unprecedented decarbonization rates or large-scale carbon removal, aligning better with current status and commitments for more plausible Earth system model inputs.


Scenarios are crucial for climate change research, guiding research communities and policymakers in exploring future pathways, evaluating temperature targets, and developing mitigation strategies<sup>1–3</sup>. Scenarios also serve as critical bridges among diverse research communities, particularly by integrating earth system models (ESMs) of the natural environment with integrated assessment models (IAMs) of socioeconomic systems<sup>4,5</sup>. This connection enables a more holistic understanding of the interactions between natural and social systems. The scenarios database of the sixth assessment report (AR6) of the Intergovernmental Panel on Climate Change (IPCC) plays a central role in assessing global warming levels, capturing diverse assumptions

about emissions, technology, socioeconomic factors, and policy interventions<sup>6,7</sup>. The five marker Shared Socioeconomic Pathways (SSP) from the Scenario Model Intercomparison Project (ScenarioMIP)—SSP1-1.9 (radiative forcing of 1.9 W (Watt) m<sup>-2</sup>), SSP1-2.6, SSP2-4.5, SSP3-7.0, and SSP5-8.5—widely used in the literature and assessed in the IPCC AR6, span a wide range of possible socioeconomic and climate futures, providing comprehensive external forcings, including emissions and atmospheric concentrations of greenhouse gases, chemically reactive gases, aerosols, and land use changes<sup>8–10</sup>.

The ScenarioMIP experiment within the Coupled Model Intercomparison Project phase 6 (CMIP6), aligned to the base year 2015<sup>9</sup>, is

<sup>1</sup>State Key Laboratory of Severe Weather Meteorological Science and Technology (LaSW), Chinese Academy of Meteorological Sciences, Beijing, China.

<sup>2</sup>Laboratory of Climate Change Mitigation and Carbon Neutrality, Henan University, Zhengzhou, China. <sup>3</sup>Institute of Energy, Environment and Economy, Tsinghua University, Beijing, China. <sup>4</sup>Tsinghua-CTG Joint Center for Climate Governance and Low-carbon Transformation, Tsinghua University, Beijing, China.

<sup>5</sup>CMA Earth System Modeling and Prediction Centre, China Meteorological Administration, Beijing, China.  e-mail: [xiaoye@cma.gov.cn](mailto:xiaoye@cma.gov.cn)

now almost a decade outdated. During this period, global carbon and pollutant emissions have experienced large changes, such as those induced by the COVID-19 pandemic and China's clean air actions and climate policies<sup>11</sup>. Additionally, major carbon-emitting countries have updated their Nationally Determined Contributions (NDCs)<sup>12,13</sup>, resulting in a significant divergence between many ScenarioMIP pathways and current realities and commitments. Two new net-zero scenarios were developed to incorporate the pandemic's impact on emissions, assuming significant reductions from 2023<sup>14,15</sup>. Nonetheless, these scenarios may increasingly diverge from the reality, as global emissions continue to rise in 2023 with no clear signs of decline. Specifically, given that China accounts for approximately one-third of global carbon emissions<sup>16–18</sup>, its carbon neutrality efforts will significantly influence global climate mitigation outcomes. The misalignment of existing scenarios with recent developments has thus reduced their relevance for accurately projecting current and future emissions trends<sup>19</sup>. For instance, a combination of bottom-up and top-down approaches in China estimates the 2020 carbon emissions from energy and industrial processes at 11.5 Gt (gigatonnes) CO<sub>2</sub><sup>20</sup>.

Existing SSP scenarios (SSP1-1.9, SSP1-2.6, and SSP2-4.5) diverge from China's observed emissions and policy targets, with discrepancies of 0–0.7 Gt CO<sub>2</sub> (2020), 0.9–5.6 Gt (2030), and –6.4–1.0 Gt (2060) relative to current estimates and pledged goals. While ScenarioMIP marker scenarios retain validity in their projection ranges, all exhibit sizeable deviations from China's documented emissions trajectory and climate targets. In addition to these discrepancies in estimates, the latest version of the Community Emissions Data System (CEDS) database, used for harmonized emissions trajectories, has substantially corrected historical data that was used in CMIP6. For instance, the global anthropogenic CH<sub>4</sub> emissions for 2015 have been revised down by 4.3%, from 373.7 in the CMIP6 release (v.2016\_07\_16) to 357.4 megatons (Mt) CH<sub>4</sub> yr<sup>–1</sup> in the latest version (v.2024\_04\_01 pre-release). Similarly, global anthropogenic volatile organic compounds (VOCs) emissions have been reduced by 16%, from 163.9 to 137.3 Mt VOC yr<sup>–1</sup>. Global black carbon (BC) emissions have decreased by 29%, from 8 to 5.7 Mt BC yr<sup>–1</sup>, and global organic carbon (OC) emissions have dropped by 32%, from 19.5 to 13.3 Mt OC yr<sup>–1</sup>.

Developing scenarios rooted in current realities that align with recent policy commitments and provide clear trajectories from the present to net-zero emissions for China and the global community is key to guiding the international efforts towards keeping the temperature goal for the Paris Agreement and reaching the Sustainable Development Goals (SDGs). Due to the rapidly evolving landscape of climate policy and technological advancements, future scenarios need to incorporate dynamic, region-specific data and consider pledges, challenges, and priorities specific to regions and countries to stay relevant. The network for greening the financial system (NGFS) scenarios have been updated with new economic and climate data, policy commitments, and model versions<sup>21</sup>, but a full set of gridded emissions data for ESM has not yet been produced. To quickly address the challenges mentioned, CMIP has launched a CMIP7 fast-track with streamlined experiments to meet specific needs, including those of the IPCC's Seventh Assessment Report (AR7)<sup>22</sup>. Creating a new version of CMIP is highly complex and requires extensive coordination and time. Therefore, we propose a simplified framework as a transitional product between CMIP6 and CMIP7 and as an additional resource before the release of the CMIP7 fast-track. Here, we present an interdisciplinary, multi-model framework (Fig. 1) that integrates up-to-date emissions data and recent national commitments to reduce greenhouse gases and air pollutants, offering a comprehensive tool for navigating the path to a sustainable future (SSP2-com). In SSP2-com, the 2 indicates that the global scenario is derived from SSP2, while com stands for combination, signifying that the scenario is constructed by integrating diverse tools, methodologies, and national, regional, and global emissions. Termed 'reality-aligned' to reflect its data-anchored

methodology, this framework integrates contemporary emissions trends and policy developments, synthesizing multi-scale data sources (AR6 database, China-specific models) to maintain consistency in sectoral-regional trajectories. Inconsistencies in sector categorization are resolved by redistributing emissions data to align with updated inventories, and global warming levels are calculated using three emulators. This framework is designed to incorporate additional sub-regional input data in the future. Detailed methodologies and data sources are outlined in Fig. 1 and the Methods section.

## Results

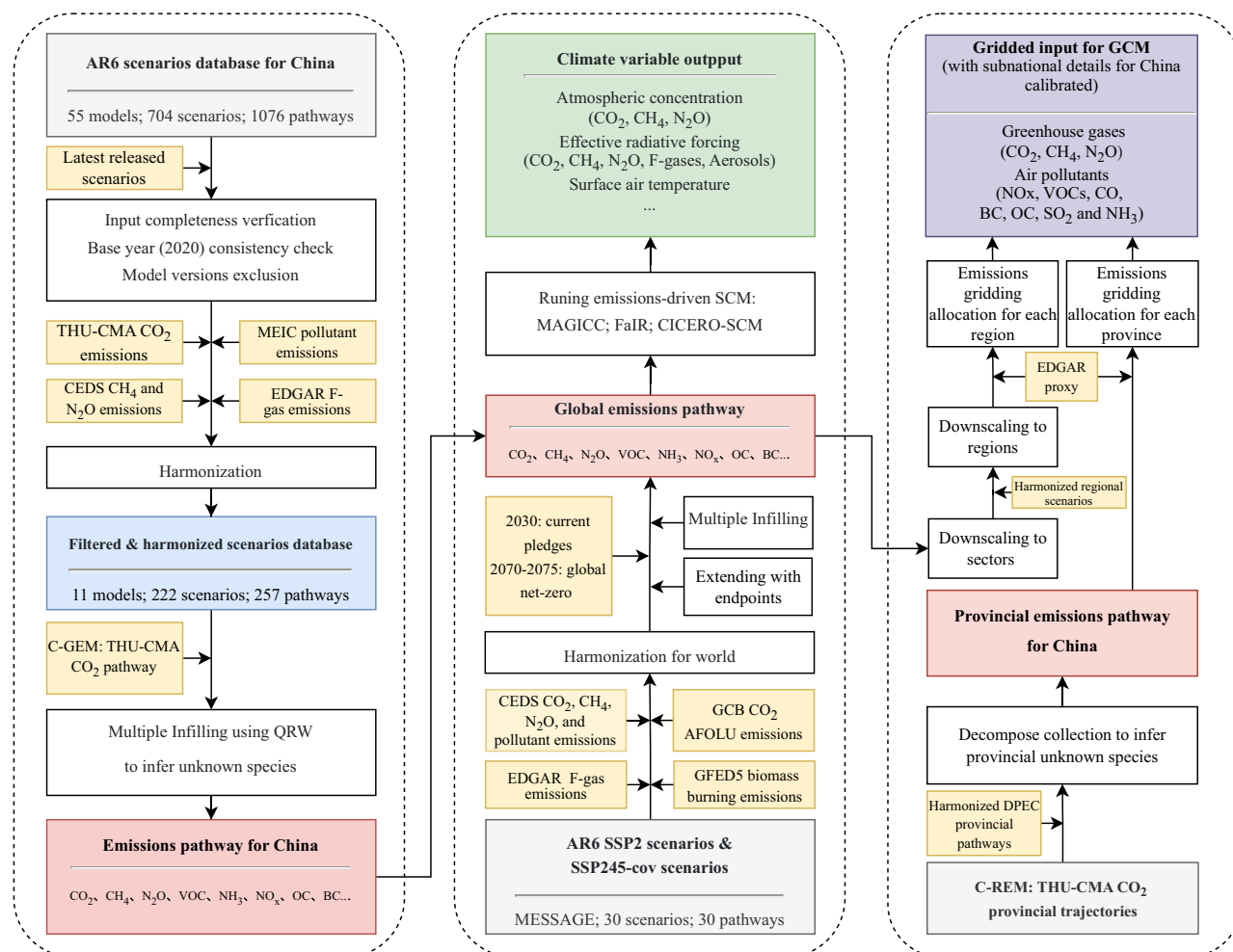
### Stated policy emissions pathway for the world and China

Figure 2 presents the future global and China's emissions pathway for key greenhouse gases and pollutants expected to contribute most significantly to global warming, along with their sectoral compositions, as a result of SSP2-com, AR6, and recent updates (projected trajectories for other greenhouse gases are provided in Supplementary Fig. 4).

For China, following the peak in carbon emissions around 2028–2029, the transition to renewable energy sources, particularly wind and solar power, is crucial for reducing carbon emissions in the energy and industrial sectors, ultimately achieving carbon neutrality by 2060. The transportation and residential/commercial sectors also contribute to this reduction from now to 2060. CH<sub>4</sub> emissions are expected to decline primarily from the energy sector, though the agriculture and waste sectors remain significant contributors through 2060. SO<sub>2</sub> emissions are projected to decrease significantly across three sectors: industrial, energy, and residential/commercial. Similarly, OC, BC, CO, and VOC emissions see substantial reductions from now to 2060, largely from industrial, transportation, and residential/commercial shifts from traditional biomass and fossil energy to cleaner energy sources. The industrial and transportation sectors mainly influence the reduction in NO<sub>2</sub> emissions by 2060. While the agricultural sector also experiences a marked decline, it continues to be a major source of NH<sub>3</sub> emissions.

### Diverse drivers at global-to-regional and national-to-provincial scales

Figure 3a illustrates the future distribution of major greenhouse gas and pollutant emissions across six key global regions under classification schemes from WGIII AR6<sup>23</sup> (Supplementary Table 2), highlighting the primary sectors and regions driving the projected decreases in total annual emissions by 2100 compared to 2020. Currently, the Asia and Pacific (APC) region is the largest contributor to global CO<sub>2</sub> emissions, accounting for approximately 49% of the global total. However, it is also projected to be the largest contributor to emissions reductions by 2100, with a decrease of approximately 17 Gt CO<sub>2</sub> yr<sup>–1</sup> (42% of global reduction), compared to current levels. The energy sector is expected to contribute the most (66%), followed by the industrial (21%) and transport (9%) sectors. The Developed Countries (DEV) region<sup>24</sup>, the second-largest source of global carbon emissions, contributing around 29%, is projected to achieve a reduction of approximately 11.7 billion tons of CO<sub>2</sub> annually by 2100 (29% of global reduction). The primary drivers of these reductions are the energy and transport sectors. While having lower carbon emissions, the Latin America and Caribbean (LAM) region ranks third in future emissions reduction potential, owing to its significant negative emissions potential. Africa (AFR) and Eastern Europe and West-Central Asia (EEA) follow, with the Middle East (ME) contributing the least. In a similar pattern to CO<sub>2</sub>, the APC region, despite being the highest emitter of CH<sub>4</sub> globally, is also expected to achieve the most significant reduction in methane emissions by 2100, with a decrease of 75 Mt CH<sub>4</sub> yr<sup>–1</sup> compared to 2020. The energy sector leads this reduction by 2100, followed by the industrial sector, with the waste sector also making a notable contribution. Currently, the DEV, LAM, and AFR regions each



**Fig. 1 | Integrated framework for emissions scenario development and climate modeling for China and the world.** (yellow blocks are input data, gray blocks are scenarios database, white blocks are methods, red blocks represent global and

China's greenhouse gas and pollutant pathway, green blocks are emulator outputs, and purple blocks represent gridded emissions for earth system models; regions represent global divisions, while provinces denote subregions in China).

contribute similarly to global CH<sub>4</sub> emissions (ranging from 14% to 17%), and their reduction contributions by 2100 are expected to be comparable. Both the industrial and energy sectors contribute positively; however, in the AFR region, the waste sector is expected to contribute negatively due to factors such as population growth and urbanization. For the seven major pollutants, the APC region, while currently the largest emitter, is also projected to contribute the most to future reductions. By 2100, annual emissions are projected to decrease by 34 Mt VOC (45% of global reduction), 20 Mt NH<sub>3</sub> (57%), 35 Mt NO<sub>2</sub> (56%), 25 Mt SO<sub>2</sub> (50%), 6 Mt OC (52%), 2.5 Mt BC (59%), and 223 Mt CO (64%). The reductions in VOC emissions primarily come from the industrial, transport, and residential/commercial sectors, while NH<sub>3</sub> reductions almost entirely come from agriculture. NO<sub>2</sub> reductions are mainly from the transport sector, SO<sub>2</sub> by the energy sector, and OC, BC, and CO reductions are predominantly from the residential and commercial sectors. The DEV region ranks second only to APC in NH<sub>3</sub> and NO<sub>x</sub> reduction contributions, while AFR ranks second to APC in OC, BC, and CO reductions.

For sub-regions and sub-national levels, more detailed carbon emission trajectories allow us to develop greenhouse gas and carbon emission trajectories, providing a more detailed depiction of the net zero scenario for each sub-region. Taking China as an example, we have derived complete regional scenarios by building on the provincial carbon emission trajectories, utilizing quantile rolling window and

time-dependent ratio techniques. Figure 3b illustrates the primary provinces and sectors driving the reduction in CO<sub>2</sub> and pollutant emissions in China by 2060 compared to 2020, with pie charts representing the share of emissions reductions attributed to the leading ten provinces relative to the total reductions across all provinces. For CO<sub>2</sub>, the largest decreases are from the energy and industrial sectors, with significant contributions from provinces like Shandong, Hebei, Inner Mongolia, and Henan. VOC reductions are predominantly led by the industrial sector, with notable contributions from Guangdong, Zhejiang, Jiangsu, and Shandong provinces. NH<sub>3</sub> reductions are almost entirely from the agricultural sector, particularly in Yunnan, Sichuan, and Henan provinces.

### Projected warming levels by 2100

Figure 4 presents the projected temperature rise, the warming level in 2100, and the cumulative years exceeding 2 °C for the SSP2-com scenario as simulated by three different climate emulators (50th percentile across all members of the full run). According to MAGICC (the Model for the Assessment of Greenhouse-gas Induced Climate Change), global surface temperature is projected to increase by 2.03 °C above pre-industrial levels by 2100, with the temperature surpassing 2 °C in 2058 and peaking at 2.10 °C in 2081 before gradually declining (Supplementary Table 3). FaIR (the Finite Amplitude Impulse Response model) estimates a slightly lower increase of 1.99 °C by 2100,

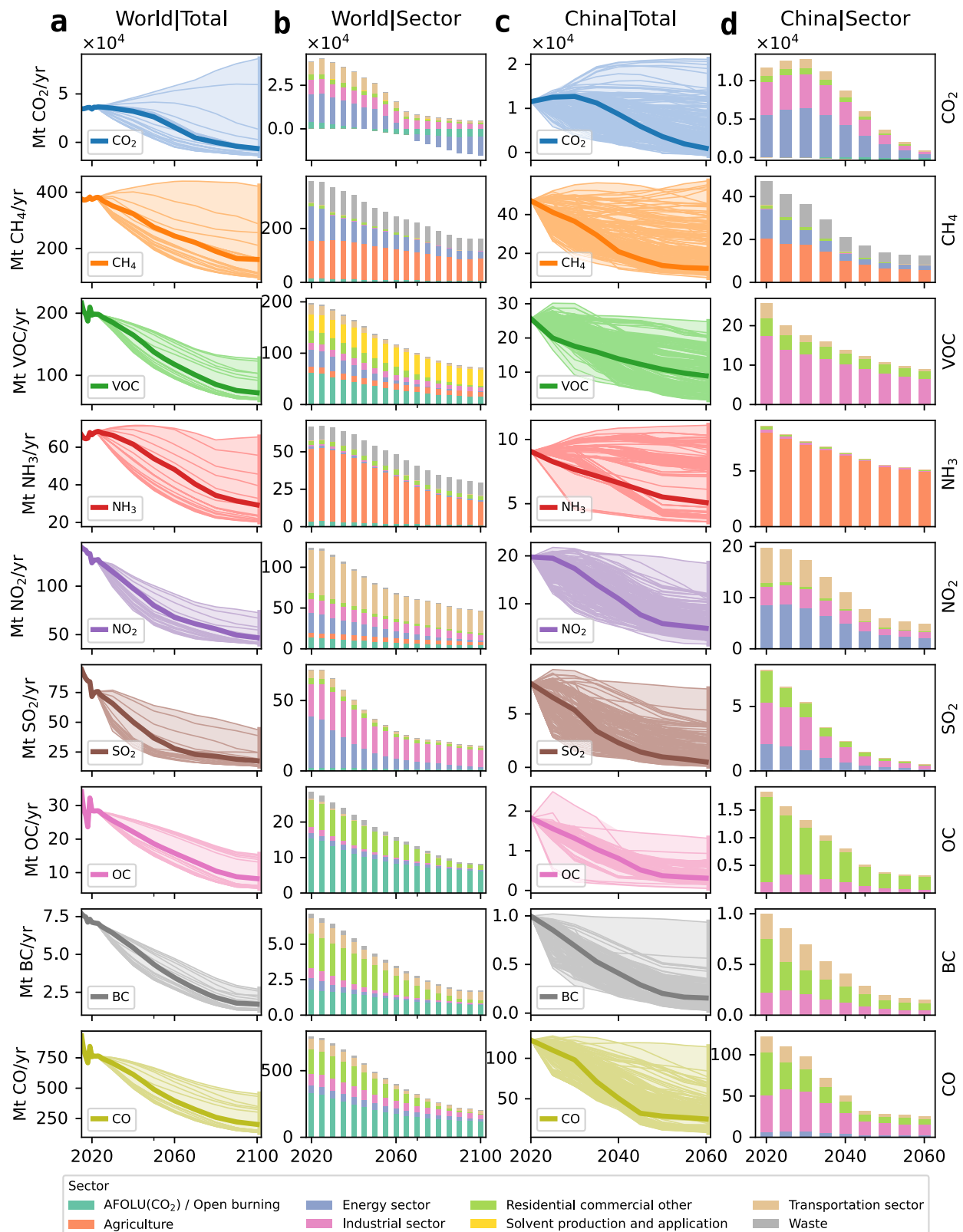


**Fig. 2 | Projected emissions pathway of key greenhouse gases and air pollutants in total and by sector for the world and China. a** Pathways in total for the world, **(b)** pathways by sector for the world, **(c)** pathways in total for China, and **(d)**

pathways by sector for China. (The solid lines in **a**, **c** represent the trajectories of SSP2-com, while the transparent lines represent the trajectories in the database).

with temperatures exceeding 2 °C as early as 2047, peaking at 2.12 °C in 2071. CICERO-SCM (the CICERO Simple Climate Model) forecasts a 2.02 °C rise by 2100, with the temperature crossing the 2 °C threshold in 2051 and peaking at 2.15 °C in 2071. Projected warming trajectories,

as estimated by three independent emulators, indicate that global temperatures are likely to reach approximately 2.01 °C above pre-industrial levels by 2100 (with consistent projections for the 2091-2100 period), relevant to the Paris Agreement's temperature target. Our

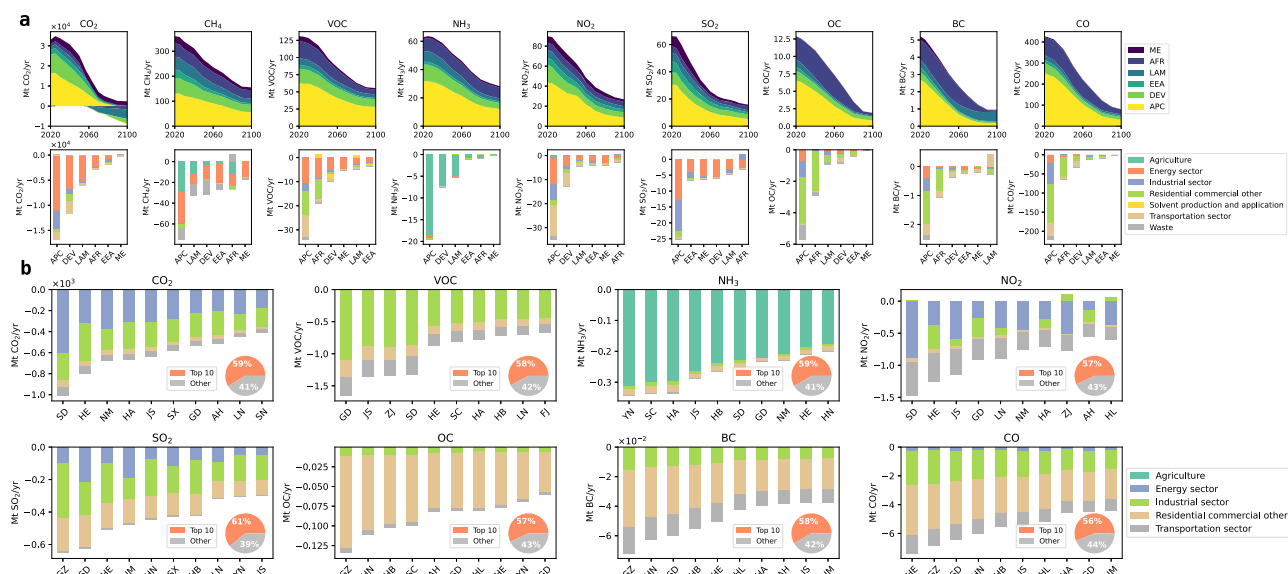


**Fig. 3 | Regional emissions pathway and sectoral emissions reductions of greenhouse gases and air pollutants. a** Time series of annual total emissions from 2100 to 2020 for six regions in the world (APC: Asia and Pacific, EEA: Eastern Europe and West-Central Asia, AFR: Africa, ME: Middle East, LAM: Latin America and the Caribbean, DEV: Developed Countries); and **(b)** Top 10 provinces in China by emissions reductions from 2020 to 2100, with pie charts showing their share of

total national reductions (SD: Shandong, HE: Hebei, NM: Inner Mongolia, HA: Henan, JS: Jiangsu, SX: Shanxi, GD: Guangdong, AH: Anhui, LN: Liaoning, SN: Shaanxi, ZJ: Zhejiang, SC: Sichuan, HB: Hubei, FJ: Fujian, YN: Yunnan, HN: Hunan, HL: Heilongjiang, and GZ: Guizhou) (Each column in a or subplot in b represents an individual species).

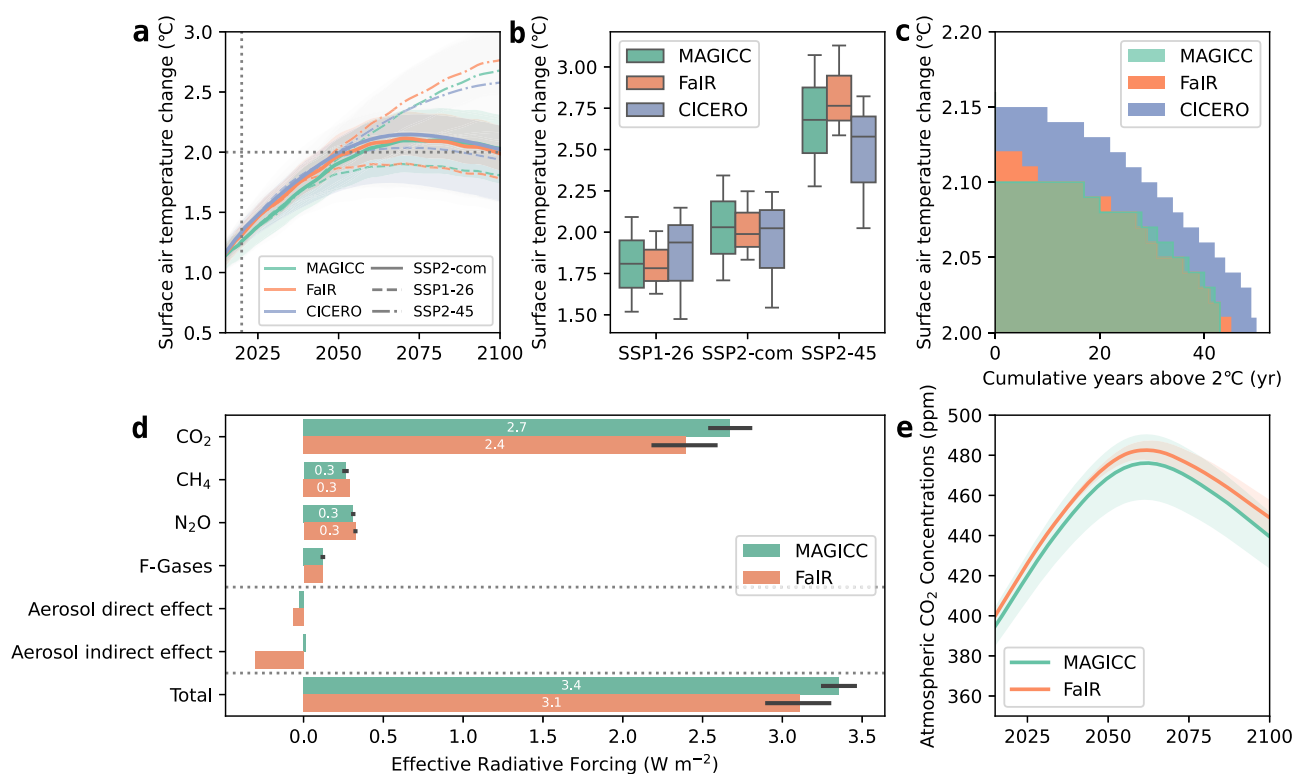


**Fig. 4 | Climate model projections of SSP2-com from three emulators: MAGICC, FaIR, and CICERO-SCM. a** Surface temperature change relative to pre-industrial levels; **(b)** temperature rise by 2100 for different scenarios; **(c)** cumulative years

above 2 °C; **(d)** effective radiative forcing of major components, and **(e)** simulated atmospheric CO<sub>2</sub> concentrations.

projected trajectories also show distinct warming patterns across adjacent decades: average temperatures for 2091–2100 are projected at 2.04 °C, while the subsequent decade (2101–2110) shows a slight decline to 1.98 °C, suggesting that the year 2100 represents a critical inflection point in the 2 °C threshold trajectory. This warming lies

between the SSP1-2.6 and SSP2-4.5 scenarios—higher than the more idealistic SSP1-2.6, yet significantly lower than SSP2-4.5.

In the SSP2-com scenario, the total radiative forcing by 2100 is around 3 W m<sup>-2</sup>, with MAGICC estimating 3.4 W m<sup>-2</sup> and FaIR 3.1 W m<sup>-2</sup>. The effective radiative forcing from CO<sub>2</sub> is the dominant contributor,



with MAGICC and FaIR estimating  $2.7 \text{ W m}^{-2}$  and  $2.4 \text{ W m}^{-2}$ , respectively.  $\text{CH}_4$  and  $\text{N}_2\text{O}$  continue to play significant roles, contributing approximately  $0.3 \text{ W m}^{-2}$ . F-gases also contribute, albeit less significantly, at around  $0.1 \text{ W m}^{-2}$ . Aerosols remain a cooling force, though the magnitude is uncertain; MAGICC suggests a near-zero direct and indirect aerosol effect, whereas FaIR estimates an indirect cooling effect of approximately  $0.4 \text{ W m}^{-2}$ . The differences between MAGICC and FaIR in simulating aerosol indirect effects likely stem from their model structures and parameterization methods. MAGICC uses a detailed physical parameterization to represent aerosol-cloud interactions<sup>25</sup>, while FaIR employs a simplified response model that relies more on historical data fitting<sup>26</sup>. By 2100, MAGICC projects the global atmospheric  $\text{CO}_2$  concentration to reach 448.9 ppm, a 61% increase from pre-industrial levels, with a peak of 482.5 ppm in 2062. FaIR projects a  $\text{CO}_2$  concentration of 439.5 ppm by 2100, reflecting a 58% increase, peaking at 476.1 ppm in 2062. The concentration changes of  $\text{CH}_4$  and  $\text{N}_2\text{O}$  are illustrated in Supplementary Fig. 5.

The temperature overshoot in SSP2-com is generally limited to a maximum of  $0.15^\circ\text{C}$ , with only a few years exceeding  $0.1^\circ\text{C}$  (about 10 years in FaIR and none in MAGICC). This suggests that very fast and deep decarbonization or rigorous carbon dioxide removal pathways, which usually entail substantially higher costs and equity concerns, may not need to be emphasized to limit warming to  $-2^\circ\text{C}$  at 2100. Given the substantial uncertainties surrounding overshoot pathways that rely on large-scale carbon removal—particularly due to over-confident model projections of Earth's response to overshoot scenarios, questionable reversibility of regional climates, and the challenges of human adaptation post-overshoot<sup>27</sup>—our scenario, with its very limited  $2^\circ\text{C}$  overshoot, offers a precautionary approach that

may help reduce these uncertainties. The temperature is expected to stabilize around  $2^\circ\text{C}$  by 2100, reducing the likelihood of triggering critical climate tipping points associated with the 2 to  $3^\circ\text{C}$  warming projected under current policies<sup>28</sup>.

### Gridded emissions bridging IAMs and ESMs

Building on the reality-aligned emissions pathway that span from global to regional and national to provincial scales, we developed a global sector-specific gridded emission dataset with a  $10 \times 10 \text{ km}$  resolution. This new dataset provides two advantages over previous gridded data. It offers a more accurate depiction of current global emissions and can incorporate updated regional and national carbon peak and neutrality pathways, thereby creating a more plausible foundation for Earth system modeling. Additionally, the high-resolution grid of  $10 \times 10 \text{ km}$  is compatible with the requirements of various global climate models (GCMs) and provides detailed initial conditions essential for high-resolution regional climate models. Figure 5 illustrates the global distribution of carbon emissions for 2020, 2060, and 2100, alongside the total and sectoral differences between 2100 and 2020. Compared to 2020, most global regions are expected to experience significant carbon emissions reductions by 2060, particularly in high-emissions areas of the Northern Hemisphere. By 2100, emissions decline consistently and markedly across all regions, with the majority achieving net-zero emissions. The most substantial reductions from 2020 to 2100 are observed in East Asia, Western Europe, North America, and South America. In East Asia, Western Europe, and North America, nearly all sectors show substantial decreases, accompanied by notable negative  $\text{CO}_2$  emissions, positioning these regions as the most critical contributors to global net-

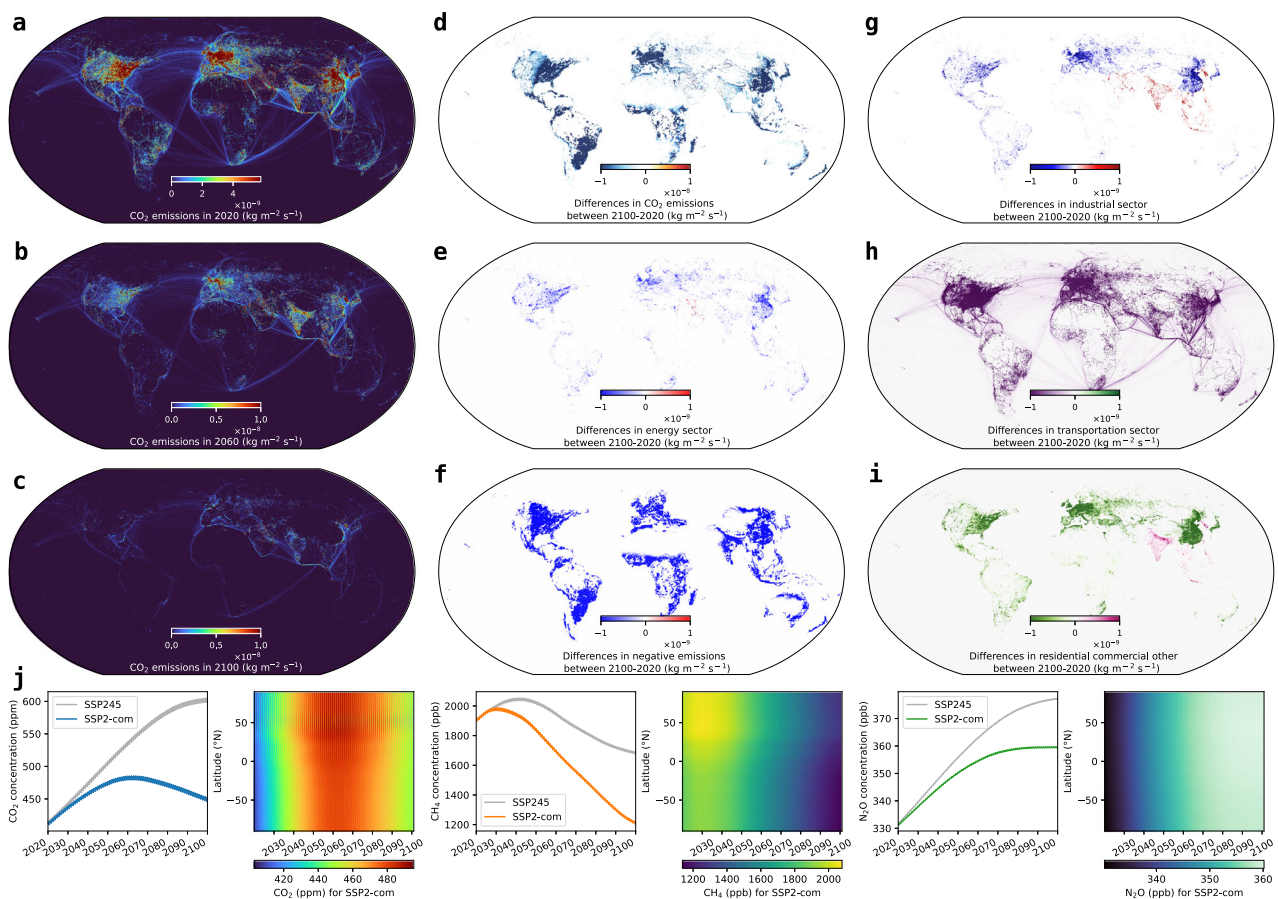


**Fig. 5 | Spatial and temporal variations in  $\text{CO}_2$  emissions.** a–c Global  $\text{CO}_2$  emissions for 2020, 2060, and 2100; (d–i) differences in total and sectoral  $\text{CO}_2$  emissions between 2100 and 2020; and (j) time series of global average and zonal distributions of  $\text{CO}_2$ ,  $\text{CH}_4$ , and  $\text{N}_2\text{O}$  concentrations.

zero targets. In South America, while absolute reductions in energy, industrial, and transportation emissions are limited, the region's significant deployment of negative emissions technologies, such as bioenergy with carbon capture and storage, plays a crucial role in global emissions reductions.

From 2020 to 2100, global CH<sub>4</sub> emissions undergo a pronounced decline, with the most significant reductions observed across East Asia, South Asia, Europe, North America, and South America (Supplementary Fig. 6). This widespread decrease is predominantly from agricultural, waste, and energy mitigation efforts. Emissions reductions in agriculture are particularly pronounced in East Asia, South Asia, South America, and Africa, where targeted interventions have substantially curbed CH<sub>4</sub> outputs. Emissions of the seven major air pollutants exhibit marked declines from 2020 to 2060, with further reductions extending to 2100, especially in regions such as East Asia and South Asia, where current pollutant levels are notably elevated (Supplementary Figs. 7–9).

We adjusted the SSP2-4.5 concentration files using MAGICC's global concentration outputs to align with the zonal distributions, to enhance their applicability in earth system modeling. Detailed global average and zonal distribution fields for CO<sub>2</sub>, CH<sub>4</sub>, and N<sub>2</sub>O concentrations are shown here. CO<sub>2</sub> and CH<sub>4</sub> concentrations are projected by MAGICC to follow a trajectory of peaking before declining. CH<sub>4</sub> is expected to peak around 2030, notably earlier than CO<sub>2</sub>, due to its comparatively shorter atmospheric lifetime and heightened sensitivity to changes in emissions. This may also contribute to the zonal distribution of global CH<sub>4</sub> concentrations, which exhibits higher levels in the Northern Hemisphere, with peak concentrations observed at mid-latitudes.

### Regional and national scenario combination framework (SSP2-com +)

A regional and national scenario integration framework, SSP2-com +, is further proposed aimed at facilitating the exchange of carbon emission trajectories that are more precisely tailored to the unique circumstances of individual regions and countries. Under this framework, each region or country is expected to provide at least one carbon emission trajectory, which is used to generate detailed greenhouse gas and pollutant trajectories. These trajectories will be integrated into the SSP2-com+ framework and re-run monthly to produce updated warming levels and gridded emissions input for ESM. To ensure the relevance and flexibility of the scenarios, the SSP2-com+ framework plans to publish updated versions every six months, thereby keeping the framework dynamic and responsive to new data and commitments.

Previous scenario update cycles were lengthy, limiting their effectiveness for timely analysis and decision-making support. This approach allows for the scenarios to be more finely tuned to the distinct environmental and socioeconomic realities of different regions and nations, significantly enhancing their policy relevance for climate change mitigation efforts. By enabling the integration of diverse data inputs and the flexibility to update scenarios as needed, the SSP2-com+ framework is poised to increase the applicability and robustness of the scenarios. The transparency and accessibility of this framework can facilitate countries, especially those lack of capacity, to propose and analyze their own and global scenarios.

### Discussion

Our study establishes an interdisciplinary, multi-model framework that integrates up-to-date emissions inventories, national commitments, and sector-specific trajectories to construct a global scenario aligned with national emissions pathways. This framework addresses critical gaps in existing scenario databases by harmonizing regional and national data across scales—global to sub-provincial—while incorporating the latest policy developments and emissions trajectories. A

potential contribution lies in its open-source and general design, which enables researchers, particularly those from nations lacking IAM capabilities, to rapidly generate emissions pathways, SCM outputs, and gridded emissions datasets for ESMs. Compared with the CMIP6 ScenarioMIP framework, which relies on decade-old baselines and requires extensive coordinating resources, our approach is lightweight, modular, and adaptable to frequent updates. We acknowledge that the CMIP6 ScenarioMIP offers comprehensive and forward-looking projections that span a wide range of socioeconomic and climatic futures. Building on this legacy, our work serves as a complementary effort to ScenarioMIP, refining its broad projections into policy-relevant, target-specific scenarios grounded in real-world developments.

The SSP2-com scenario, derived from this framework, provides a suite of outputs, including an emissions pathway, SCM projections, and high-resolution gridded inputs for ESMs. Notably, it incorporates subnational details for China, calibrated to reflect provincial-level emissions trajectories and sectoral contributions, offering detailed granularity in scenario development. Our global scenario is derived from strictly selected SSP2 emissions scenarios to inherit SSP2 assumptions and updated 2022/2023 baselines and global and China's NDCs. Our scenario's warming targets are higher than SSP1-2.6, but significantly lower than SSP2-4.5 (Supplementary Fig. 12). Initially, our temperature trajectory closely follows SSP2-4.5, but it aligns more closely with SSP1-2.6's trends post-2050. By 2100, our scenario closely aligns with SSP1-2.6, predicting temperatures about 0.2 °C higher. Unlike SSP1-2.6, which ensures that warming does not exceed 2 °C annually by 2100, our scenario shows small but sustained overshoots of 2 °C, with temperature over 2.1 °C for about 10 years in FaIR and none in MAGICC. Since these overshoots are comparatively minor, our scenario may obviate the need for extensive deployment of negative emissions technologies in the near term to sequester CO<sub>2</sub>. Thus, our scenario is closely aligned with currently stated ambitions and still avoids a high overshoot of 2 °C. This will mitigate the potential risks associated with overshoot, including triggering strong Earth system feedbacks, leading to sustained warming in both the near and long term<sup>27</sup>. Regarding atmospheric CO<sub>2</sub> concentrations (Supplementary Fig. 13), our future concentration trajectory mirrors that of SSP1-2.6, first rising and then declining, with the gap between the two peaks around 2060 before narrowing. This trajectory starkly contrasts the continuous rise observed in SSP2-4.5, SSP3-7.0, and SSP5-8.5, without following a steep decline depicted in SSP1-1.9. Compared to the 2015 commitments, the probability of exceeding 4 °C in global mean surface temperature change by 2100 is significantly reduced under both the updated pledges-continued ambition and updated pledges-enhanced ambition scenarios<sup>29</sup>, while the likelihood of constraining temperature change below 2 °C and 1.5 °C is substantially enhanced<sup>29</sup>. Current policy trajectories project a median warming of 2.6 °C by century's end<sup>30</sup>. When incorporating both high- and low-confidence net-zero targets, this median projection decreases to 2.0 °C<sup>30</sup>, aligning with the SSP2-com warming level. This convergence suggests that strengthened climate commitments could effectively reduce the anticipated temperature rise relative to current policy implementations. Compared with NGFS scenarios (Supplementary Fig. 3), the SSP2-com scenario results in higher cumulative emissions by 2080 compared to Low Demand, Net Zero 2050, Below 2 °C, and Delayed Transition scenarios, with stronger negative emissions after 2080. SSP2-com has a slower near-term emissions decline but accelerates decarbonization post-2050, surpassing NDCs and Fragmented World scenarios, which show continued temperature increases. In contrast, SSP2-com stabilizes warming by -2070, followed by a decline, highlighting the importance of early, coordinated climate action compared to the slower reductions under Current Policies.

The framework's flexibility is further demonstrated through its SSP2-com+ extension, which allows six-month updates of regional and

national pathways. This contrasts with the multi-year revision cycles of CMIP6 and NGFS, ensuring scenarios remain responsive to evolving policies and technological breakthroughs. For example, integrating China's provincial-level trajectories—which account for heterogeneous economic and industrial profiles—enhances the spatial accuracy of global gridded emissions data. Such granularity is absent in most existing scenarios, which often homogenize regional dynamics.

Some uncertainties of our work are also acknowledged here. Our scenario construction, which spans provincial, regional, and global scales, incorporates data from multiple sources. These databases harbor inherent uncertainties that, when coupled with cross-mapping between source categories, introduce additional complexities. Despite these uncertainties, rigorous efforts have been made to align these diverse data sources to minimize discrepancies. Additionally, uncertainties arise during the harmonization and infilling processes for different species, regions, and sectors' emission trajectories. To mitigate these errors, we adhere to the CMIP6 input protocol<sup>14,9,15</sup>. A further source of uncertainty is the grid allocation process. We distribute grids globally, across six major regions down to China's provinces, without accounting for inter-regional variability within other regions outside Asia. The SSP2-com+ scenario will incorporate pathways from additional countries and regions, thereby enhancing the granularity of regional variations within the framework.

Despite these challenges, our scenario has made progress in plausibly approaching the specifics of the global and national current status and commitments. The produced gridded data have been used by several ESMs, including BCC-CSM and CESM2, to assess the levels of global warming, future losses and damages, and impacts on extreme events, overshoot, and tipping points. Gridded emission data will be updated in a timely manner, as our scenario framework incorporates the emissions pathway from more countries, particularly developing countries<sup>24</sup> and at subnational levels, which will better serve future IPCC assessment cycles, climate negotiations, and international mitigation actions<sup>31</sup>.

## Methods

### Scenario database from AR6 and recent updates

The AR6 Scenario Database is a pivotal integral resource to the IPCC's Sixth Assessment Report<sup>32</sup>. This database collects, harmonizes, and assesses scenarios from various integrated assessment models, climate models, and impact assessment models across the globe. The AR6 Scenario Database facilitates an in-depth understanding of climate futures based on various assumptions regarding greenhouse gas emissions, technological advancements, socioeconomic factors, and policy decisions. This database comprises a comprehensive collection of global to national-level energy, emissions, and sector scenarios spanning from September 2019 to July 2021, encompassing 189 models, 1,389 scenarios, 1,791 variables, and 244 regions.

This study integrates two additional scenarios (SSP245-cov) that account for the impact of the COVID-19 pandemic on emissions<sup>15</sup> into our infilling database. The moderate green scenario anticipates a moderate investment increase in green and low-carbon technologies post-2023, targeting a 35% reduction below NDCs by 2030 and achieving net-zero CO<sub>2</sub> emissions by 2060. The strong green scenario envisages a significant increase in such investments, aiming for the same 52% reduction below NDCs by 2030 and achieving net-zero CO<sub>2</sub> emissions by 2050. Additionally, the scenarios FossilFuel and TwoYearBlip in SSP245-cov are also included in the database.

The recently updated scenario data from Cheng, Tong<sup>33</sup> are also added to our infilling database for China. Specifically, the scenarios include baseline, clean air, on-time peak-clean air, on-time peak-net zero-clean air, and early peak-net zero-clean air. These scenarios were developed using the Global Change Assessment Model (GCAM-China) and the dynamic projection model for emissions in China (DPEC). In these scenarios, emissions from the heating sector were categorized

into the industrial sector rather than the energy sector, creating inconsistencies with other inventories. To address this, we adjusted the emissions by redistributing the heating sector's data to the energy sector based on the relative proportion of heating and industrial emissions from a detailed 22-sector inventory. For CO<sub>2</sub> emissions, we further aligned the data using the newly released harmonized inventory<sup>17</sup>, ensuring consistency across all sectors.

According to the unconditional commitments set by NDCs, carbon emissions are projected to increase by 1% in 2025 and decrease by 2% in 2030 (relative to 2019)<sup>34</sup>, which is close to SSP2. The SSP2 scenario (MESSAGE) and the latest SSP245-cov scenario (30 pathways in total) were selected from the AR6 global scenario database for global scenarios (Supplementary Table 1). For China's scenarios, 257 pathways were selected from the AR6 scenario database and recent updates from Cheng, Tong<sup>33</sup> after integrity checks, consistency checks, and removal of old versions (Supplementary Method 1).

### THU-CMA CO<sub>2</sub> emission trajectory for China and provinces

For this study, we incorporated projected CO<sub>2</sub> emissions in China from Zhang, Huang<sup>20</sup>. The THU-CMA (Tsinghua University-China Meteorological Administration) trajectory, developed by an economy-wide computable equilibrium model, the China-in-Global Energy Model (C-GEM)<sup>35</sup>, outlines a comprehensive CO<sub>2</sub> emissions reduction strategy for China. The trajectory suggests that China's CO<sub>2</sub> emissions peak around 2028–2029 at approximately 12.8 GtCO<sub>2</sub>. Following this peak, emissions are projected to decline to about 11.2 GtCO<sub>2</sub> by 2035, further decreasing to 3.6 GtCO<sub>2</sub> by 2050 and ultimately reaching 0.9 GtCO<sub>2</sub> by 2060 (Supplementary Fig. 10). This scenario integrates both bottom-up emissions factor methods and top-down atmospheric CO<sub>2</sub> concentration inversion methods<sup>16</sup>, ensuring a robust and cross-validated approach. Additionally, the trajectory aligns with China's updated NDCs, which aim to peak CO<sub>2</sub> emissions before 2030 (achieve carbon neutrality before 2060). It also incorporates economic considerations, projecting a cumulative GDP cost of approximately 0.9% between 2020 and 2060. This scenario is instrumental in evaluating China's potential to achieve carbon neutrality while adhering to the 2 °C global temperature rise limit. Given that the carbon emissions in 2060 under the THU-CMA trajectory fall between the SSP1-1.9 and SSP1-2.6 scenarios, the post-2060 emissions trajectory for China was derived by taking the average of the emissions pathways from these two scenarios. This approach provides a balanced representation of potential future emissions, aligning the THU-CMA trajectory with established low-carbon scenarios.

We also utilized provincial-level CO<sub>2</sub> emission trajectories<sup>36</sup>, which provide detailed emission trajectories for 30 provinces, aligning with the national THU-CMA trajectory. These trajectories were developed using the China Regional Energy Model (C-REM) to assess the economic impacts of the proposed scenarios. C-REM is a recursive-dynamic, multi-sector, and multi-region computable general equilibrium model that captures China's economic and energy systems with high granularity at the provincial level<sup>37</sup>. It shows that China's CO<sub>2</sub> emissions peak around 2028–2029 at about 12.8 GtCO<sub>2</sub>, with significant contributions from major emitting provinces such as Shandong, Hebei, Inner Mongolia, Jiangsu, Guangdong, and Shanxi<sup>38</sup> (Supplementary Fig. 11). By downscaling the national trajectory to the provincial level, this study provides a comprehensive framework for understanding regional contributions to China's carbon neutrality goals. The detailed provincial trajectories facilitate targeted policy development and academic research, ensuring that mitigation strategies are tailored to the specific circumstances of each province.

### Historical emissions data

CEDS offers a comprehensive dataset of global anthropogenic emissions for various pollutants and greenhouse gases from 1750



onwards<sup>39</sup>. Developed by the Joint Global Change Research Institute, CEDS integrates numerous regional and sector-specific inventories, providing consistent emissions data for climate and air quality modeling. The system's robust methodology includes historical data reconstruction, making it a critical resource for understanding long-term emissions trends and their impacts on climate change. Its latest release in April 2024 updates driver and emissions data, extending the emissions time series to 2022. Major features include updated default data from IEA, Energy Institute, and EDGAR, refined country inventories, extended liquid fuel data, and expanded representation of the metal smelting sector.

The Emissions Database for Global Atmospheric Research (EDGAR), managed by the European Commission's Joint Research Center, delivers detailed global emissions data for various air pollutants and greenhouse gases<sup>40–42</sup>. Covering various sectors, including energy, industry, and agriculture, EDGAR combines data from international, national, and regional inventories. It employs a uniform methodology to ensure comparability across regions and periods, making it indispensable for policy analysis, scientific research, and international climate assessments. EDGARv8.0, developed by the JRC and IEA, offers estimates of CO<sub>2</sub>, CH<sub>4</sub>, N<sub>2</sub>O, and fluorinated gases by sector and country. The newest version, EDGARv8.1, spans from 1970 to 2022 and includes emissions data for ozone precursor gases (CO, NO<sub>2</sub>, NMVOC, CH<sub>4</sub>), acidifying gases (NH<sub>3</sub>, NO<sub>2</sub>, SO<sub>2</sub>), and primary particulates (PM<sub>10</sub>, PM<sub>2.5</sub>, BC, OC).

The Multi-resolution Emission Inventory for China (MEIC) is an advanced emissions inventory system that provides high-resolution data on air pollutants and greenhouse gases, specifically for China<sup>43</sup>. Developed by Tsinghua University, MEIC incorporates data from numerous Chinese sources, offering detailed temporal and spatial resolution. The latest update, version 1.4, released in May 2023 by the MEIC team, now spans from 1990 to 2020, covering key sectors such as power, industry, transport, residential, and agriculture, and includes 22 sub-sectors. It tracks emissions of pollutants, including SO<sub>2</sub>, NO<sub>2</sub>, CO, NMVOC, NH<sub>3</sub>, PM<sub>2.5</sub>, BC, OC, and CO<sub>2</sub>.

The Global Carbon Budget (GCB) is an annual evaluation of the sources and sinks of CO<sub>2</sub>, produced by the Global Carbon Project. It provides estimates of emissions from fossil fuel combustion, cement production, land-use changes, and natural carbon sinks in oceans and terrestrial ecosystems. In the 2023 edition<sup>44</sup>, the GCB includes detailed data on CO<sub>2</sub> emissions from the Agriculture, Forestry, and Other Land Use (AFOLU) sector, which has been adopted for this study.

The Global Fire Emissions Database (GFED5) offers a detailed record of biomass burning emissions worldwide, integrating satellite observations with biogeochemical models<sup>45,46</sup>. GFED5 provides data on fire emissions' temporal and spatial distribution, including various greenhouse gases and aerosols. The database is essential for studying the role of fires in the carbon cycle, climate system, and air quality. It supports research on fire dynamics, land-atmosphere interactions, and the impacts of fire emissions on global and regional scales. The current version, GFED5, offering a spatial resolution of 0.25 degrees covering the years 2002 through 2020, was used in this study.

### Harmonizing emissions pathways

In our study, we utilize the open-source software Aneris to automate emissions harmonization<sup>47</sup>, aligning model outputs with a standardized historical emissions dataset to ensure seamless transitions into future projections. This process is critical for the accuracy of global climate models, which depend on the continuity of emissions and concentration fields. Harmonization adjusts model outputs to a specified base year while addressing discrepancies caused by different underlying datasets. Aneris selects appropriate methods—ratio and offset or convergence techniques—based on the differences between model results and historical data, ensuring that both regional details and sector-specific dynamics are accurately represented. This

methodological framework supports the integrity of model projections and facilitates the detailed analysis of emissions pathways across diverse global activities. All harmonization is based on the following equations, where  $\beta$  is the harmonization convergence parameter in Eq. (1),  $m^{rat}$  is the ratio-based harmonization in Eq. (2),  $m^{off}$  is the offset-based harmonization in Eq. (3), and  $m^{int}$  is the linear-interpolation-based harmonization in Eq. (4). Each equation is a function of historical and model trajectories, base year ( $t_i$ ), convergence year ( $t_f$ ), at which point the harmonized trajectory converges to the unharmonized trajectory.

$$\beta(t, t_i, t_f) = \begin{cases} 1 - \frac{t-t_i}{t_f-t_i}, & \text{if } t \leq t_f \\ 0, & \text{otherwise} \end{cases} \quad (1)$$

$$m^{rat}(t, m, h, t_i, t_f) = \left[ \beta(t, t_i, t_f) \left( \frac{h(t_i)}{m(t_i)} - 1 \right) + 1 \right] m(t) \quad (2)$$

$$m^{off}(t, m, h, t_i, t_f) = \beta(t, t_i, t_f) (h(t_i) - m(t_i)) + m(t) \quad (3)$$

$$m^{int}(t, m, h, t_i, t_f) = \begin{cases} \frac{m(t_f)-h(t_i)}{t_f-t_i} (t-t_i) + h(t_i), & \text{if } t \leq t_f \\ m(t), & \text{otherwise} \end{cases} \quad (4)$$

Since 2020 in AR6 database is an estimated year, and the emissions database, including CEDS, EDGAR, and GFED5, has been updated to varying degrees, there are discrepancies in the baseline year 2020 that need to be aligned (Supplementary Figs. 14–15).

To ensure consistency in global emissions data, we adopt the CEDS database to align CO<sub>2</sub>, CH<sub>4</sub>, and pollutant emissions due to previous practice from CMIP6 ScenarioMIP and its approximation of ensemble averages, as shown in IPCC WGIII reports<sup>32</sup>. In the CMIP6 scenarios, 2015 is established as the baseline year using CEDS v2016. However, the 2024 update to the CEDS significantly revised historical emissions data (Supplementary Fig. 16). Updating historical data could help refine the alignment, enhancing the accuracy and relevance of the projections. The latest report from the International Energy Agency (IEA) shows a 1.1% year-on-year increase in global energy-related CO<sub>2</sub> emissions in 2023. This growth rate informs the update of CEDS global carbon emissions from 2022 to 2023. In addition, CEDS emissions cover 61 sectors, differing from IAM model classifications, and both are unified into ten categories as specified by ScenarioMIP, including agriculture, energy, industrial processes, transportation, residential, Commercial, and other sectors, solvents production and application, waste, international shipping, aircraft, and biomass burning. Since CEDS does not include fluorinated greenhouse gas emissions, we adopt the EDGAR database used in IPCC AR6 (latest EDGAR 8.0, updated to 2022) for alignment with emissions of 12 types of fluorinated gases. For fire emissions, CMIP6 uses GFED4, but GFED4 has been updated to GFED5 (latest in 2020), which shows global carbon emissions 60% higher than previous versions. To maintain consistency with CMIP6, we align GFED5 with GFED4 using average values from 2004–2014 (with details provided in the Supplementary Method 2). The IPCC AR6 references the GCB 2020 report, which estimated average annual carbon emissions from global AFOLU at 5.9 billion tons of CO<sub>2</sub> for 2010–2019 and 6.6 billion tons in 2019. However, the GCB 2023 report revised the 2019 figure to 4.6 billion tons, aligning with GCB 2022 data. To ensure consistency in China's emissions data, THU-CMA CO<sub>2</sub> emissions, CEDS CH<sub>4</sub> and N<sub>2</sub>O emissions, MEIC pollutant emissions, and EDGAR F-gas emissions are used (Supplementary Fig. 18).

Adopting the alignment method consistent with CMIP6 ScenarioMIP, specific methods are selected based on different criteria.

Overall, our approach involves harmonizing emissions for 3 major greenhouse gases (CO<sub>2</sub>, CH<sub>4</sub>, N<sub>2</sub>O), 7 pollutants (NO<sub>2</sub>, SO<sub>2</sub>, VOC, NH<sub>3</sub>, OC, BC, and CO), and 12 halogenated greenhouse gases, using databases including THU-CMA CO<sub>2</sub> Emissions, CEDS, MEIC, and EDGAR (Supplementary Figs. 17–18). The harmonization year for global carbon emissions and pollutants is 2022, while the harmonization year for China's carbon emissions and pollutants is 2020.

### Extending with endpoints

Our global scenario follows the CMIP7 Scenario MIP proposal for a 2°C low scenario. This scenario maintains current commitments until 2030 and aims to achieve global net-zero CO<sub>2</sub> emissions around 2070. According to the unconditional commitments set by NDCs, carbon emissions are projected to increase by 1% in 2025 and decrease by 2% in 2030, relative to 2019 levels<sup>34</sup>. These projections establish the global carbon emissions totals for 2025 and 2030. For post-2030 carbon emissions, we employ the quantile time projection method, using 30 pathways in total from the SSP2 MESSAGE scenarios and the latest SSP245-cov scenario (see Supplementary Method 3). This method assumes that an emissions trajectory maintains a fixed quantile in the filled database, allowing us to extend its time series from the last available data point (2030). By applying this technique, we obtained the global carbon emission trajectory for 2030–2100. We slightly adjusted the projected trajectory to align with the goal of achieving net-zero CO<sub>2</sub> emissions around 2070, resulting in a comprehensive future global carbon emissions scenario (Supplementary Fig. 19).

### Infilling missing emissions species

The Quantile Rolling Window (QRW) technique processes time series by segmenting them into rolling windows and performing quantile calculations within each window to derive relationships. The quantile rolling window technique is stable and suitable for large-scale databases. It has already been applied in the AR6 WGIII report and SSP245-cov scenario production<sup>15,48</sup>. The QRW method includes rolling window determination, normalized distance calculation, weights calculation, and cumulative weights calculation. First, the time series is divided into multiple windows, each with a central position on the timeline. The windows can overlap, and both the width of each window and the interval between their central positions can be adjusted according to specific needs. Second, the normalized distance ( $d_n$ ) is calculated based on Eq. (5), where  $f$  is a decay factor,  $b$  is the distance between window centers.

$$d_n = \frac{x - x_{\text{window}}}{f \times \left(\frac{b}{2}\right)} \quad (5)$$

Thirdly, data points are weighted in each window based on the weights ( $\omega(x, x_{\text{window}})$ ) calculated from Eq. (6), with those farther from the center of the window receiving lower weights.

$$\omega(x, x_{\text{window}}) = \frac{1}{1 + (d_n)^2} \quad (6)$$

Finally, we calculate the cumulative weights ( $c_w$ ) and then the cumulative sum up to half weights ( $c_{hw}$ ) based on Eqs. (7–8), where  $\omega$  is the raw weight.

$$c_w = \sum_{i=1}^n \omega_i \quad (7)$$

$$c_{hw} = c_w - 0.5 \times \omega \quad (8)$$

Utilizing the QRW technique, we derived future emissions trajectories for CH<sub>4</sub>, N<sub>2</sub>O, AFOLU, 7 pollutants, and 12 halogenated

greenhouse gases for both China and the world (see Supplementary Method 7). For global projections, the future emissions trajectories were obtained from 30 pathways from the SSP2 MESSAGE scenarios and the latest SSP245-cov scenario. For China, the future emissions pathway was derived from selected 257 pathways from the AR6 scenario database and recent updates. China's emissions pathway extended further into 2100 (Supplementary Fig. 20).

### Climate emulators

To assess the warming levels within our global scenario, we employed three emulators to obtain effective radiative forcing, surface temperature increase, and atmospheric concentrations of greenhouse gases. These three emulators include MAGICC, FaIR, and CICERO-SCM. The MAGICC model is an advanced and highly configurable climate model emulator that has been influential in climate policy and research discussions<sup>25</sup>. Version 7.5.3 of MAGICC continues its tradition of providing projections of global temperatures and other climatic variables under various greenhouse gas emissions scenarios. This version features updated calibrations based on the IPCC WGI report and includes enhanced ocean and carbon cycle feedback modules. MAGICC is renowned for its ability to simulate historical climate data and project future changes, informing national policy-making and international climate agreements.

The FaIR model focuses on the relationship between global temperatures and atmospheric concentrations of greenhouse gases, aerosols, and other forcing agents<sup>26,49</sup>. It is designed to quickly estimate the Earth's temperature response to emissions scenarios with relatively few input parameters and is also evaluated as highly accurate, similar to MAGICC, by WGI cross-chapter box 7.1. FaIR v1.6.4 includes updates that improve aerosol forcing calculations and compatibility with the latest emissions databases. Its simplicity and speed make it a popular tool for educational purposes and integrated assessment models, which aids in rapid policy analysis and feedback.

CICERO-SCM model version 1.1.2 is developed by the Center for International Climate Research in Oslo<sup>50</sup>. This streamlined climate model emulator focuses on replicating the essential dynamics between greenhouse gas emissions, atmospheric concentrations, radiative forcing, and temperature change. The latest version includes refined algorithms that better mimic complex climate feedback mechanisms and interactions with the carbon cycle. CICERO-SCM is particularly valued for its user-friendly interface and the inclusion of scenarios that align with the latest IPCC reports, making it a practical choice for policymakers and researchers alike who need quick yet reliable climate projections.

We used an open-source software package (OpenSCM-Runner)<sup>51</sup>, designed for streamlined climate model simulations, to conduct our experiments. This enabled us to perform a series of experiments involving three distinct parameter sets across three climate models (OpenSCM-Runner or the official default). Each set of experiments was designed to explore the sensitivity and responses of the models to varying levels of climate sensitivity and other parameters.

### Regional Downscaling from global to regional and national to provincial scales

The time-dependent ratio method establishes the connection between two variables by positing that the dependent time series is the product of the independent time series and a time-varying scaling factor. This factor is calculated as the ratio of the dependent variable to the independent variable. When numerous such variable pairs exist in the database, the scaling factor is determined by the ratio of their average values. The infilling process is conducted based on Eq. (9), where  $E_f(t)$  is emissions of the infilling variable,  $E_l(t)$  is the leading variable, and  $R(t)$ , the scaling factor calculated from Eq. (10), is the ratio of the

means of the infilled and the leading variables.

$$E_f(t) = R(t) \times E_l(t) \quad (9)$$

$$R(t) = \frac{\text{mean}(e_f(t))}{\text{mean}(e_l(t))} \quad (10)$$

In this study, we developed a methodology to align and downscale emissions data from various sectors within the SSP2 scenario database, utilizing historical data and time-dependent ratio techniques. Specifically, we downscaled global greenhouse gas and pollutant emissions from 2022 to 2100 by sector to six major regions as defined in the IPCC WGI AR6 (Supplementary Table 2). We establish the relationship between aggregate variables and their constituent components, whose sum should be equal to the time series of the aggregate, and then use this to deconstruct aggregate variables in our scenario. This allowed us to track the changes in emissions across nine species categories in the different regions from 2022 to 2100.

Further refining our scale of analysis, we applied the THU-CMA provincial carbon emission trajectories aligned with the DPEC pathways to break down these emissions from the country level to the province. Using quantile rolling window and time-dependent ratio techniques, we obtained detailed provincial and sectoral emissions trajectories.

### Emissions gridding

We detail the emissions gridding allocation for each global region and every province in China, adhering to the CMIP6 gridding protocol<sup>8</sup>. Initially, emissions at the sector level are apportioned across various global regions—DEV, EEA, LAM, AF, ME, APC without China, and China (CN). This regional data is then mapped onto a spatial grid using the EDGAR grid proxy data.

The allocation process distributes emissions into specific grid cells ( $x, y$ ) according to Eq. (11), where:

$$Emis(x, y) = Emis_{reg} \times \frac{\text{proxyvalue}(x, y)}{\sum \text{proxyvalue}(x, y)} \quad (11)$$

where  $Emis(x, y)$  represents the emissions value for grid cell ( $x, y$ ),  $Emis_{reg}$  is the total emissions for the region at the sector level,  $\text{proxyvalue}(x, y)$  denotes the proxy data value for cell ( $x, y$ ), and the summation extends over all coordinates within the specified region. The proxy data values are adjusted for each region by scaling according to the fractional area of each grid cell located within the region, which is calculated annually. This methodology ensures that grid cells spanning multiple countries proportionally allocate emissions based on the proxy data's spatial distribution.

The methodology is similarly applied to each province within China, following the same detailed procedure described for global regions. This ensures that emissions data are accurately gridded at a more localized level, allowing for nuanced analysis and reporting of emissions within each province in China. Each provincial dataset undergoes the same rigorous allocation process using province-specific EDGAR grid proxy data. This is crucial for accurately reflecting the diverse economic and industrial activities across provinces, thus providing a precise spatial distribution of emissions within China. The formula used for allocation remains consistent, ensuring methodological coherence across all geographical scales. It's noted that this approach has inherent limitations, as future changes across different regions and grid cells are unlikely to evolve synchronously.

In the default gridded historical and future emissions data, emissions from power generation and extensive industrial facilities are often represented as major point sources. However, this approach introduces inconsistencies when modeling future net-negative CO<sub>2</sub> emissions. In reality, CO<sub>2</sub> is removed from the atmosphere at biofuel

production sites, not at point sources. Therefore, representing net-negative CO<sub>2</sub> emissions as point absorptions is inaccurate and can lead to errors in ESM simulations, potentially resulting in unrealistically low or even negative CO<sub>2</sub> concentration values<sup>8</sup>. To address the allocation of negative emissions in the energy sector, we utilized the global grid map of potential biofuel productivity from CMIP6. This approach distributes the total negative emissions from the energy sector across grid cells for the six global regions, including China. By aligning the allocation with areas of potential biofuel productivity, this method ensures a more accurate representation of where CO<sub>2</sub> removal occurs within the global energy system.

To align with ESM requirements, sectoral and gridded VOC emissions were further allocated into the 23 subcategories used in CMIP6. This process involved interpolating the VOC subcategories from the SSP2-4.5 scenario to a 0.1° resolution and calculating the proportions of each component. These proportions were then used to allocate VOC emissions in the current scenario, ensuring consistency with CMIP6 categorization and enhancing the model's emissions representation accuracy.

As a result, we constructed sector-specific emissions data at a 0.1° × 0.1° resolution for three greenhouse gases (CO<sub>2</sub>, CH<sub>4</sub>, N<sub>2</sub>O), seven pollutants (NO<sub>2</sub>, SO<sub>2</sub>, BC, OC, VOC, NH<sub>3</sub>, CO), and 23 VOC species under the SSP2-com scenarios. To accommodate the requirements of various global and regional models, the data were also aggregated to a 0.5° × 0.5° resolution, ensuring compatibility across different modeling frameworks (Supplementary Fig. 21).

### Concentration data

Considering that most models utilize latitudinally distributed, well-mixed greenhouse gases, we adjusted the SSP2-4.5 concentration files based on global concentration values output by MAGICC. This modification ensures that our projections align with the latitude-specific distributions commonly used in climate modeling, providing a more accurate representation of CO<sub>2</sub>, CH<sub>4</sub>, and N<sub>2</sub>O concentrations across different geographical regions.

### Data availability

Data supporting the findings of this study are openly available in several repositories. The IPCC AR6 database can be accessed at <https://data.ece.iiasa.ac.at/ar6/>, and the CMIP6 data are available at <https://esgf-node.llnl.gov/projects/cmip6/>. Additionally, various inventory data used in this study are sourced from the respective official homepages. The scenario SSP2-com developed in this study, which includes complete trajectories of future emissions of greenhouse gases and pollutants, climate variable outputs from three emulators, and gridded inputs for GCMs, has been made publicly available (<https://doi.org/10.5281/zenodo.14906554>).

### Code availability

All computation and visualization were performed using Python and its third-party libraries (Python Software Foundation: Python Language Reference, version 3.9.13, available at <http://www.python.org>). The scenario construction and analysis utilized a suite of Python libraries designed explicitly for integrated assessment and climate data manipulation, including Pyam (<https://github.com/IAMconsortium/pyam>), Silicone (<https://github.com/GranthamImperial/silicone>), Aneris (<https://github.com/iiasa/aneris>), Scmdata (<https://github.com/openscm/scmdata>), and Openscm (<https://github.com/openscm/openscm-runner>). The code for constructing scenario frameworks and plotting has been open-sourced at <https://zenodo.org/uploads/14906555>.

### References

1. Moss, R. H. et al. The next generation of scenarios for climate change research and assessment. *Nature* **463**, 747–756 (2010).



2. Riahi, K. et al. The shared socioeconomic pathways and their energy, land use, and greenhouse gas emissions implications: an overview. *Glob. Environ. Change* **42**, 153–168 (2017).
3. O'Neill, B. C. et al. Achievements and needs for the climate change scenario framework. *Nat. Clim. Change* **10**, 1074–1084 (2020).
4. O'Neill, B. C. et al. The scenario model intercomparison project (ScenarioMIP) for CMIP6. *Geosci. Model Dev.* **9**, 3461–3482 (2016).
5. Tebaldi, C. et al. Climate model projections from the scenario model intercomparison project (ScenarioMIP) of CMIP6. *Earth Syst. Dyn.* **12**, 253–293 (2021).
6. Peters, G. P., Al Khourdajie, A., Sognaes, I. & Sanderson, B. M. AR6 scenarios database: an assessment of current practices and future recommendations. *npj Clim. Action* **2**, 31 (2023).
7. Cointe, B. The AR6 scenario Explorer and the history of IPCC Scenarios Databases: evolutions and challenges for transparency, pluralism and policy-relevance. *npj Clim. Action* **3**, 3 (2024).
8. Feng, L. et al. The generation of gridded emissions data for CMIP6. *Geosci. Model Dev.* **13**, 461–482 (2020).
9. Gidden, M. J. et al. Global emissions pathways under different socioeconomic scenarios for use in CMIP6: a dataset of harmonized emissions trajectories through the end of the century. *Geosci. Model Dev.* **12**, 1443–1475 (2019).
10. IPCC. Climate Change 2021: The Physical Science Basis. Contribution of Working Group I to the Sixth Assessment Report of the Intergovernmental Panel on Climate Change (eds Masson-Delmotte, V. et al.). (Cambridge University Press, Cambridge, UK and New York, NY, USA, 2021).
11. Wang, Z. et al. Incorrect Asian aerosols affecting the attribution and projection of regional climate change in CMIP6 models. *npj Clim. Atmos. Sci.* **4**, 2 (2021).
12. Zhao, W. China's goal of achieving carbon neutrality before 2060: experts explain how. *Natl. Sci. Rev.* **9**, nwac115 (2022).
13. Wei, Y.-M. et al. Policy and management of carbon peaking and carbon neutrality: a literature review. *Engineering* **14**, 52–63 (2022).
14. Forster, P. M. et al. Current and future global climate impacts resulting from COVID-19. *Nat. Clim. Change* **10**, 913–919 (2020).
15. Lamboll, R. D. et al. Modifying emissions scenario projections to account for the effects of COVID-19: protocol for CovidMIP. *Geosci. Model Dev.* **14**, 3683–3695 (2021).
16. Zhong, J. et al. Ongoing CO<sub>2</sub> monitoring verify CO<sub>2</sub> emissions and sinks in China during 2018–2021. *Sci. Bull.* **68**, 2467–2476 (2023).
17. Xu, R. et al. MEIC-global-CO<sub>2</sub>: A new global CO<sub>2</sub> emission inventory with highly-resolved source category and sub-country information. *Sci. China Earth Sci.* **67**, 450–465 (2024).
18. IEA, CO<sub>2</sub> Emissions in 2022, IEA, Paris <https://www.iea.org/reports/co2-emissions-in-2022>, Licence: CC BY 4.0 (2023).
19. Vo, T. P. T. et al. Influence of the COVID-19 pandemic on climate change summit negotiations from the climate governance perspective. *Sci. Total Environ.* **878**, 162936 (2023).
20. Zhang, D. et al. A representative CO<sub>2</sub> emissions pathway for China toward carbon neutrality under the Paris Agreement's 2 °C target. *Adv. Clim. Change Res.* **14**, 941–951 (2023).
21. Richters, O. et al. NGFS Climate Scenarios Data Set (5.0) [Data set]. Zenodo. <https://doi.org/10.5281/zenodo.13989530> (2024).
22. Dunne, J. P. et al. An evolving coupled model intercomparison project phase 7 (CMIP7) and fast track in support of future climate assessment. *EGU sphere* **2024**, 1–51 (2024).
23. IPCC. Annex II: Definitions, Units and Conventions. (eds Al Khourdajie, A. et al.) <https://doi.org/10.1017/9781009157926.021> (Cambridge University Press, Cambridge, UK and New York, NY, USA, 2022).
24. IPCC Secretariat. Guidance on developed and developing countries categories. IPCC Event Manager Document INF. 2, 6 (2023).
25. Meinshausen, M., Raper, S. C. B. & Wigley, T. M. L. Emulating coupled atmosphere-ocean and carbon cycle models with a simpler model, MAGICC6 – Part 1: Model description and calibration. *Atmos. Chem. Phys.* **11**, 1417–1456 (2011).
26. Leach, N. J. et al. FalRv2. 0.0: a generalized impulse response model for climate uncertainty and future scenario exploration. *Geosci. Model Dev.* **14**, 3007–3036 (2021).
27. Schleussner, C.-F. et al. Overconfidence in climate overshoot. *Nature*. **634.8033**, 366–373 (2024).
28. Armstrong McKay, D. I. et al. Exceeding 1.5 °C global warming could trigger multiple climate tipping points. *Science* **377**, eabn7950 (2022).
29. Ou, Y. et al. Can updated climate pledges limit warming well below 2 °C?. *Science* **374**, 693–695 (2021).
30. Rogelj, J. et al. Credibility gap in net-zero climate targets leaves world at high risk. *Science* **380**, 1014–1016 (2023).
31. Zhang, X. et al. China can achieve carbon neutrality in line with the Paris agreement's 2 °C target: navigating global emissions scenarios, warming levels, and extreme event projections. *Engineering* **44**, 207–214 (2025).
32. IPCC. Climate Change 2022: Mitigation of Climate Change. Contribution of Working Group III to the Sixth Assessment Report of the Intergovernmental Panel on Climate Change (eds Shukla, P. R.) <https://doi.org/10.1017/9781009157926> (Cambridge University Press, Cambridge, UK and New York, NY, USA, 2022).
33. Cheng, J. et al. A synergistic approach to air pollution control and carbon neutrality in China can avoid millions of premature deaths annually by 2060. *One Earth* **6**, 978–989 (2023).
34. UNFCCC Secretariat. 2023 NDC Synthesis Report. UNFCCC. <https://unfccc.int/ndc-synthesis-report-2023> (2024).
35. Zhang, X. et al. Research on the pathway and policy of energy economy transition under the goal of carbon neutrality. *Manag. World* **38**, 35–66 (2022).
36. Peng, H.-T. et al. Representative CO<sub>2</sub> emissions pathways for China's provinces toward carbon neutrality under the Paris Agreement's 2 °C target. *Adv. Clim. Change Res.* **15**, 1096–1106 (2024).
37. Peng, H., Qu, C., Karplus, V. J., Zhang, D. The C-REM 4.0 model: a CGE model for provincial analysis of China's carbon neutrality target. *Energy Clim. Manag.* **1**, 9400006 (2025).
38. Guo, L. et al. Construction and application of a regional kilometer-scale carbon source and sink assimilation inversion system (CCMVS-R). *Engineering* **33**, 263–275 (2024).
39. Hoesly, R. M. et al. Historical (1750–2014) anthropogenic emissions of reactive gases and aerosols from the Community Emissions Data System (CEDS). *Geosci. Model Dev.* **11**, 369–408 (2018).
40. Crippa, M. et al. CO<sub>2</sub> emissions of all world countries - 2022 Report. Publications Office of the European Union, (2022).
41. Crippa, M. et al. Gridded emissions of air pollutants for the period 1970–2012 within EDGAR v4.3.2. *Earth Syst. Sci. Data* **10**, 1987–2013 (2018).
42. Janssens-Maenhout, Greet. EDGARv4.2 Emission Maps. European Commission, Joint Research Centre (JRC) [Dataset] PID: <http://data.europa.eu/89h/jrc-edgar-emissionmaps42> (2011).
43. Zheng, B. et al. Mapping anthropogenic emissions in China at 1 km spatial resolution and its application in air quality modeling. *Sci. Bull.* **66**, 612–620 (2021).
44. Friedlingstein, P. et al. Global Carbon Budget 2023. *Earth Syst. Sci. Data* **15**, 5301–5369 (2023).
45. Randerson, J. T. et al. Global fire emissions database, version 4.1 (GFEDv4). ORNL Distributed Active Archive Center (DAAC) dataset. <https://doi.org/10.3334/ORNLDAAC/1293> 2017: 1293 (2017).
46. Chen, Y. et al. Multi-decadal trends and variability in burned area from the fifth version of the Global Fire Emissions Database (GFED5). *Earth Syst. Sci. Data* **15**, 5227–5259 (2023).
47. Gidden, M. J. et al. A methodology and implementation of automated emissions harmonization for use in Integrated Assessment Models. *Environ. Model. Softw.* **105**, 187–200 (2018).



48. Kikstra, J. S. et al. The IPCC Sixth Assessment Report WGIII climate assessment of mitigation pathways: from emissions to global temperatures. *Geosci. Model Dev.* **15**, 9075–9109 (2022).
49. Millar, R. J., Nicholls, Z. R., Friedlingstein, P. & Allen, M. R. A modified impulse-response representation of the global near-surface air temperature and atmospheric concentration response to carbon dioxide emissions. *Atmos. Chem. Phys.* **17**, 7213–7228 (2017).
50. Sandstad, M. et al. CICERO Simple Climate Model (CICERO-SCM v1.1.1) – an improved simple climate model with a parameter calibration tool. *EGUosphere* **2024**, 1–51 (2024).
51. Nicholls, Z. et al. OpenSCM-Runner: thin wrapper to run simple climate models (emissions driven runs only). GitHub Repos. (2021).

## Acknowledgements

This work was supported by the National Natural Science Foundation of China (42341202 & 42205152). The authors are grateful to all the organizations and groups that provided indispensable datasets that we used in this work and extend our sincere gratitude to Gerrit Hansen for her significant comments to this work.

## Author contributions

X.Y.Z. conceived the study and supervised the research. J.Z. conducted model development, data analysis, and manuscript writing. D.Z. developed the socioeconomic scenarios and provided the THU-CMA CO<sub>2</sub> emission pathway for China. H.P., X.H., and C.Q. provided the provincial CO<sub>2</sub> emission trajectories. D.W. and L.G. performed regional and national scale analyses. Z.W., Y.D.L., and Y.X.L. advised on ESM input requirements. X.L.Z. and C.M. guided policy interpretation and contributed to framework design. X.Y.Z., J.Z., D.Z., D.W., L.G., H.P., X.H., Z.W., Y.D.L., Y.X.L., C.Q., X.L.Z., and C.M. reviewed the manuscript and approved the final version.

## Competing interests

The authors declare no competing interests.

## Additional information

**Supplementary information** The online version contains supplementary material available at <https://doi.org/10.1038/s41467-025-62983-5>.

**Correspondence** and requests for materials should be addressed to Xiaoye Zhang.

**Peer review information** *Nature Communications* thanks Jarmo Kikstra, Ryna Yiyun, and the other, anonymous, reviewer(s) for their contribution to the peer review of this work. A peer review file is available.

**Reprints and permissions information** is available at <http://www.nature.com/reprints>

**Publisher's note** Springer Nature remains neutral with regard to jurisdictional claims in published maps and institutional affiliations.

**Open Access** This article is licensed under a Creative Commons Attribution-NonCommercial-NoDerivatives 4.0 International License, which permits any non-commercial use, sharing, distribution and reproduction in any medium or format, as long as you give appropriate credit to the original author(s) and the source, provide a link to the Creative Commons licence, and indicate if you modified the licensed material. You do not have permission under this licence to share adapted material derived from this article or parts of it. The images or other third party material in this article are included in the article's Creative Commons licence, unless indicated otherwise in a credit line to the material. If material is not included in the article's Creative Commons licence and your intended use is not permitted by statutory regulation or exceeds the permitted use, you will need to obtain permission directly from the copyright holder. To view a copy of this licence, visit <http://creativecommons.org/licenses/by-nc-nd/4.0/>.

© The Author(s) 2025